Food and Chemical Toxicology 127 (2019) 143–155

Contents lists available at ScienceDirect

Food and Chemical Toxicology

journal homepage: www.elsevier.com/locate/foodchemtox

Camptothecin induces mitotic arrest through Mad2-Cdc20 complex by activating the JNK-mediated Sp1 pathway

Matharage Gayani Dilshara[a], Rajapaksha Gedara Prasad Tharanga Jayasooriya[b], Wisurumuni Arachchilage Hasitha Maduranga Karunarathne[a], Yung Hyun Choi[c], Gi-Young Kim[a,*]

[a] Department of Marine Life Science, Jeju National University, Jeju, 63243, Republic of Korea
[b] Department of Bioprocess Technology, Faculty of Technology, Rajarata University of Sri Lanka, Mihintale, 50300, Sri Lanka
[c] Department of Biochemistry, College of Oriental Medicine, Dong-Eui University, Busan, 47227, Republic of Korea

ARTICLE INFO

Keywords:
Camptothecin
Topoisomerase I
Mitotic arrest
Tubulin
Mad2

ABSTRACT

Camptothecin (CPT) is a popular therapeutic agent that targets topoisomerase I. Our findings demonstrated that CPT-induced microtubule polymerization results in markedly increased histone H3 phosphorylation. CPT also enhanced interactions between the mitotic checkpoint proteins, Mad2 and Cdc20, and thereby increased mitotic arrest. Transient knockdown of *Mad2* completely restored cell cycle progression from CPT-induced mitotic arrest, while simultaneously reduced cyclin B1 and Cdk1 expression. Moreover, we found that c-Jun N-terminal kinase (JNK) acts upstream of Sp1, which upregulates p21-mediated mitotic arrest in response to CPT; furthermore, knockdown of *p21* restored cell cycle progression, while inhibition of Cdks completely restored cell cycle progression from CPT-induced mitotic arrest. We hypothesized that, during mitotic arrest in response to CPT, cell survival signaling blocks apoptosis, thereby enhancing mitotic arrest. As expected, a caspase-9 inhibitor, z-LEHD-FMK, and an autophagy inhibitor, 3-methyladenine (3 MA), significantly diminished CPT-induced mitotic arrest. On the other hand, when *Mad2* was depleted, z-LEHD-FMK and 3 MA markedly increased apoptosis, and restored cell cycle progression. Taken together, these results suggest that CPT decodes the action of topoisomerase I-mediated tubulin targeting drugs, leading to mitotic arrest by upregulating Mad2 through the JNK-mediated Sp1 pathway and autophagy formation from tubulin polymerization.

1. Introduction

Spindle assembly checkpoints (SACs) delay the cell cycle until all duplicated chromosomes align and attach to the spindle, which guarantees genomic stability during mitosis (Marston and Wassmann, 2017). Once mitotic spindles tightly bind to kinetochores through tubulin polymerization, from prometaphase to metaphase, the spindle assembly checkpoints are inactivated, which allows tubulin depolymerization at anaphase (Wang et al., 2014). When microtubule polymerization and depolymerization are incorrectly regulated, kinetochores trigger the SAC signaling pathway, which halts the cell cycle in the mitotic phase. Therefore, microtubule-targeting strategies that disrupt or hyperstabilize spindle microtubules have been anti-mitotic therapeutics used to treat various cancers. In particular, microtubule polymerization inhibitors, such as colchicine and vinblastine, and microtubule depolymerization inhibitors, such as paclitaxel, are extensively used to bind to tubulins. This binding disrupts microtubule dynamics and induces mitotic phase arrest (Senese et al., 2017). Additionally, recent studies have focused on the successful use of microtubule-targeting drugs in clinical trials, because their mechanism of action differs from that of other DNA-targeting drugs (Field et al., 2014; Tsimberidou et al., 2011). In fact, SACs cause cell cycle arrest at the mitotic phase in response to specific signals from kinetochores that are unable to bind to spindle microtubules due to the lack of attachment sites or improper tension imposed on sister kinetochores (Musacchio, 2015). In particular, improper tension generates the catalytic site for Mad2, which inhibits the onset of anaphase by sequestering cell-division cycle protein 20 (Cdc20) to suppress the anaphase promoting complex (APC) (Ge et al., 2009). Interactions among components of the mitotic checkpoint complex, such as the interaction between Mad2 and Cdc20, inhibit the APC-mediated ubiquitination of securin and cyclin B1 (Tian et al., 2012).

Cyclin-dependent kinases (Cdks) are associated with different stages of the cell cycle, whereas cyclins regulate the cell cycle by inducing nuclear localization, phosphorylation, and dephosphorylation of the Cdks as well as degradation of regulatory cyclin subunits (Dash and El-

* Corresponding author.
E-mail address: immunkim@jejunu.ac.kr (G.-Y. Kim).

https://doi.org/10.1016/j.fct.2019.03.026
Received 8 May 2018; Received in revised form 8 March 2019; Accepted 12 March 2019
Available online 15 March 2019
0278-6915/

Deiry, 2005). Cyclins and Cdks bind to p21 through the N-terminal CRRL consensus site, which is required to inhibit cell cycle progression (Jang et al., 2016). In particular, $p21^{-/-}$ mice have markedly decreased numbers of mitotic phase embryonic fibroblast cells with cyclin B1 expression, which suggests that p21 promotes late G_2/M phase arrest by regulating cyclin B1-Cdk1 activity (Jang et al., 2016). The induction of chromosomal instability by depletion of Mad2 reduces the availability of properly oriented metaphase chromosomes, thereby activating c-Jun-N-terminal kinase (JNK) signaling to circumvent the chromosomal instability induced by spindle checkpoint defects (Wong et al., 2014). The activation and phosphorylation of JNK, in turn, regulates stability of the transcription factor Sp1 during mitosis (Chuang et al., 2008). In response to Sp1-mediated transcription, phosphorylated p21 binds to cyclin B1 and Cdk1. The subsequent phosphorylation of Cdk1 at Thr^{161} stabilizes the binding of Cdk1 to the p21/cyclin B1 complex. (Dash and El-Deiry, 2005; Kim et al., 2014). Additionally, transient knockdown of *cyclin B* and *Cdk1* halts cells in mitotic phase. Similarly, treatment with the tubulin polymerization inhibitor, nocodazole, or the tubulin depolymerization inhibitor, paclitaxel, also regulates G_2/M phase by strongly inducing cyclin B1 and Cdk1 (Chadebech et al., 2000; Dash and El-Deiry, 2005). Choi et al. (2011) reported that selective knockdown of *Mad2* resulted in the degradation of cyclin B1 at G_2/M stage cells treated with nocodazole; whereas the accumulation of cyclin B1 and Cdk1 triggers chromosomal condensation and segregation in prometaphase arrested cells.

Xiao et al. (2003) reported that camptothecin (CPT) induces S and G_2 phase arrest through activation of Chk1 and causes the rapid proteolysis of Cdc25A, whereas knockdown of *Chk1* abrogates S phase and protects Cdc25A from degradation. CPT also induces apoptosis in cancer cells through miR-125b-mediated mitochondrial pathways by targeting the 3′-UTR regions of *p53*, *Bak1*, and *Mcl1* (Zeng et al., 2012). Nevertheless, little is known about the molecular action of CPT on G_2/M phase. In peculiar, prostate cancer is one of the most common cancer in men. Androgen-independent prostate cancer LNCaP cells are sensitive to CPT. Therefore, in the current study, we investigated the underlying molecular mechanisms of CPT activity on mitotic phase in LNCaP cells. We found that CPT-induced mitotic phase arrest is regulated by the Mad2-Cdc20 complex through the JNK-mediated Sp1 pathway and autophagy formation, resulting from tubulin polymerization.

2. Materials and methods

2.1. Reagents and antibodies

CPT, 3-(4,5-dimethylthiazol-2-yl)-2,5-diphenyltetrazolium bromide (MTT), propidium iodide, Cdk inhibitor (CdkI), paclitaxel (Tax), nocodazole (Noc), 3-methyladenine (3 MA), and z-LEHD-FMK were purchased from Sigma (St. Louis, MO) and an enhanced chemiluminescence (ECL) kit was purchased from Amersham (Arlington Heights, IL). RPMI 1640 medium, fetal bovine serum (FBS), and antibiotics mixture were purchased from WelGENE (Daegu, Republic of Korea). Antibodies against Cdc20, Mad2, β-actin, cyclin B1, JNK, Cdk1, Sp1, nucleolin, p21, phosphor (p)-21, α-tubulin (polymeric), caspase-9, caspase-8, and Bax were purchased from Santa Cruz Biotechnology (Santa Cruz, CA). Antibodies against p-histone 3 (p-H3), p-JNK, JNK, p-c-Jun, p-PTEN, and PTEN were purchased from Cell Signaling Technology (Beverly, MA). Peroxidase-labeled donkey anti-rabbit and sheep anti-mouse immunoglobulin were purchased from KOMA Biotechnology (Seoul, South Korea).

2.2. Cell culture

LNCaP cells (below 20 passages) were obtained from the American Type Culture Collection (Manassas, VA). The cells were cultured in RPMI 1640 medium supplemented with 10% FBS and antibiotics mixture at 37 °C in a 5% CO_2-humidified incubator in the presence or absence of CPT.

2.3. Flow cytometric analysis

DNA was stained with PI and then mitotic cells were quantified by measuring the expression of a mitotic-specific marker p-H3 or Mad2. In brief, LNCaP cells were trypsinized, washed three times with PBS, fixed with ice-cold 70% ethanol for overnight, and immunostained with a rabbit anti-p-H3 or anti-Mad2 antibody followed by a FITC-conjugated goat anti-rabbit antibody. The cells were then stained with PI in PBS containing 1% Triton X-100 and RNase A. p-H3 or Mad2 levels and the DNA content of individual cells were analyzed using a FACSCalibur flow cytometer (Becton Dickenson, San Jose, CA).

2.4. Western blot analysis

Whole-cell lysates were prepared by PRO-PREP protein extraction solution (iNtRON Biotechnology, Sungnam, Republic of Korea). Cytoplasmic and nuclear protein extracts were prepared using NE-PER nuclear and cytosolic extraction reagents (Pierce, Rockford, IL). The cell lysates were harvested from the supernatant after centrifugation at 13,000 *g* for 20 min. Total cell proteins were separated on polyacrylamide gels and transferred them the nitrocellulose membranes. The membranes were developed using an ECL reagent.

Isolation of total RNA and reverse transcriptase-polymerase chain reaction (RT-PCR)

Total RNA was isolated from LNCaP cells using Easy-Blue (iNtRON Biotechnology) according to the manufacturer's instruction. RNA extracts was reverse-transcribed by M-MLV reverse transcriptase kit (BioNEER, Daejeon, Republic of Korea). In brief, cDNA synthetic was amplified via PCR using specific primer *GAPDH* (forward 5′-TAC TAG CGG TTT TAC GGG CG-3′ and reverse 5′-TCG AAC AGG AGG AGC AGA GAG CGA-3′), *p21* (forward 5′-GTA AAT CCT TGC CTG CCA GA -3′ and reverse 5′-GGC TCC ACA AGG AAC TGA CT-3′) and *Mad2* (forward 5′-CAT CCA CGC TGT TTT GAC CTC ACG-3′ and reverse 5′-GGC TTT CTG GGA CTT TTC TCT-3′). The following PCR conditions were used: *GAPDH*, 27 cycles of denaturation at 94 °C for 30 s, annealing at 60 °C for 30 s, and extended at 72 °C for 30 s; *Mad2*, 32 cycles of denaturation at 94 °C for 30 s, annealing at 57 °C for 30 s, and extended at 72 °C for 30 s; *p21*, 28 cycles of denaturation at 94 °C for 30 s, annealing at 59 °C for 30 s, and extended at 72 °C for 30 s.

2.5. Immunoprecipitation (Hirota et al.)

LNCaP cells were lysed in RIPA buffer containing 1 mM phenylmethylsulfonyl fluoride and protein inhibitor cocktail. After preclearing, antibodies were added for overnight and protein A/G agarose was added and gently inverted for 1 h. After centrifugation, the resin was washed with IP lysis/wash buffer (Thermo Scientific). Bound proteins were separated by 10% SDS-PAGE gel electrophoresis and then analyzed by western blot analysis.

2.6. Small interfering RNA (siRNA)

LNCaP cells were seeded on a 24-well plate at a density of 1×10^5 cells/ml and transfected with *Mad2*-, *JNK*-, and *p21*-targeted silencing RNA (siRNA, Santa Cruz Biotechnology) for 48 h. For each transfection, 450 μl growth medium was added to 20 nM siRNA duplex with the transfection reagent G-Fectin (Genolution Pharmaceuticals Inc., Seoul, Republic of Korea) and the entire mixture was added gently to the cells.

2.7. Cdk1 kinase activity

Cdk1 kinase activity was measured by instructor's protocol

(MESACUP Cdk1 kinase assay kit, MBL International Corporation, Woburn, MA). After the cells treated with CPT for 24 h, samples were mixed with reaction mixture for 30 min. The absorbance of each well was taken at 492 nm using ELISA plate reader.

2.8. Immunofluorescence staining and confocal microscopy

LNCaP cells were seeded on glass coverslips and incubated with or without CPT at 37 °C for 24 h, washed twice with PBS, and fixed with 90% methanol at 37 °C for 30 min. The cells were washed with PBS, blocked in 10% normal goat serum for 1 h, and incubated with anti-α-tubulin antibody (1:200, Santa Cruz Biotechnology) overnight at 4 °C. Primary antibody was removed by washing the membranes in PBS containing 0.3% Triton-X (v/v) and incubated for 1 h with Alexa 488-conjugated secondary antibody (1:200, Molecular Probes, Eugene, OR). Fluorescent signals were imaged using a confocal laser scanning microscope.

2.9. Electrophoretic mobility shift assay (EMSA)

Transcription factor-DNA binding activity assays were carried out with nuclear protein extract. Synthetic complementary Sp1 (5′-ATT CGA TCG GGG CGG GCC GAG C-3′, Santa Cruz Biotechnology) binding oligonucleotides was 3′-biotinylated utilizing the biotin 3′-end DNA labeling kit (Pierce) according to the manufacturer's instructions, and annealed for 30 min at 37 °C. Samples were loaded onto native 4% polyacrylamide gels pre-electrophoresed for 60 min in 0.5× Tris borate/EDTA (TBE) buffer on ice, in the presence of transferred onto a positively charged nylon membrane (Hybond^{TM}-N+) in 0.5× TBE buffer at 100 V for 1 h on ice. The transferred DNA-protein complex was cross-linked to the membrane at 120 mJ/cm^2. Horseradish peroxidase-conjugated streptavidin was utilized according to the manufacturer's instructions to monitor the transferred DNA-protein complex.

2.10. Tubulin polymerization in vitro assay

Five mg/ml pure tubulin (Cytoskeleton, Denver, CO) were brought to a steady state G-PEM buffer [100 mM PIPES (pH 6.9), 1 mM EGTA, 1 mM $MgCl_2$, and 1 mM GTP] plus 10% glycerol in a 96-well plate by incubation at 37 °C for 1 h. The effects on polymerization/depolymerization were quantified by measuring the absorbance at 340 nm (A_{340}) with time.

2.11. Biding of FITC-phalloidin to actin polymer

LNCaP cells were treated with CPT for the indicated time points and washed twice with prewarmed PBS (pH 7.4). The cells were fixed in 3.7% formaldehyde solution for 10 min and washed twice with PBS. The cells stained with phalloidin-FITC at a concentration of 0.05 mg/ml to determine the amount of F-actin. Next, the cells were analyzed using a FACSCalibur flow cytometer.

2.12. Statistical analysis

The images were visualized with Chemi-Smart 2000 (VilberLourmat, Marine, Cedex, France). Images were captured using Chemi-Capt (VilberLourmat) and transported into Photoshop. All bands were shown a representative obtained in three independent experiments and quantified by Scion Imaging software (http://www.scioncorp.com). Statistical analyses were conducted using SigmaPlot software (version 12.0) Values were presented as mean ± standard error (S.E.). Significant differences between the groups were determined using the unpaired Student's *t*-test and one-way ANOVA with Bonferroni's test. Statistical significance was regarded at *, $^\#$, †, and ‡, $p < 0.05$.

3. Results

3.1. Mad2 is a key factor in CPT-induced mitotic phase arrest

To determine whether CPT regulates cell cycle arrest, as shown in a previous study (Xiao et al., 2003), we analyzed the cell cycle progression of LNCaP cells. The number of cells in G_2/M phase significantly increased in a time-dependent manner in response to CPT, whereas G_1 phase markedly decreased (Fig. 1A). In particular, the cell cycle arrested in S phase at 12 h after treatment with 2 μM CPT and reached G_2/M phase arrest at 24 h. Nevertheless, apoptotic sub-G_1 phase cells were not observed in the presence of CPT, suggesting that CPT potently induced G_2/M phase arrest after a short-stop at S phase, but did not induce apoptosis. To determine whether G_2 phase or mitotic phase was regulated, we monitored H3 phosphorylation because H3 is phosphorylated on Ser^{10} during early mitosis to facilitate chromatin condensation, a hallmark of the mitotic phase (Hirota et al., 2005). We detected significant levels of intracellular H3 phosphorylation at 24 h, which indirectly suggested that CPT-induced G_2 phase arrests at 18 h, followed by mitotic phase arrest at 24 h (Supplementary Fig. 1A). Western blot analysis confirmed that H3 started reductant phosphorylation on Ser^{10} at 18 h, and that the phosphorylated H3 reached maximum level at 24 h (Supplementary Fig. 1B). Next, we investigated the possibility that CPT regulates Mad2 expression, because Mad2 monitors the attachment of the kinetochore to the spindle at mitotic phase, and Mad2 levels increase when kinetochores are unattached (Saitoh et al., 2005). Similar to CPT-induced mitotic phase arrest (Fig. 1A) and H3 phosphorylation (Supplementary Figs. 1A and 1B), CPT induced the accumulation of intracellular Mad2, which started at 12 h and reached maximum levels at 24 h. This result suggested that the increase in Mad2 levels is a consequence of cell cycle arrest or is required to regulate mitotic phase arrest (Supplementary Fig. 1C). We also found that CPT caused a gradual increase of Mad2 protein (Fig. 1B) and mRNA (Fig. 1C) expression. Because, like Mad2, Cdc20 is a key component of the spindle checkpoint machinery that ensures proper attachment of sister chromosomes to kinetochores at metaphase (Tian et al., 2012), we tested for interactions between Cdc20 and Mad2. CPT markedly enhanced formation of the Mad2 and Cdc20 complex at 12 h in LNCaP cells (Fig. 1D). To further understand the functional role of Mad2 in CPT-induced mitotic phase arrest, endogenous levels of Mad2 were transiently knocked-down by *Mad2*-targeted siRNA (siMad2). Transient knockdown of *Mad2* significantly downregulated Mad2 expression (Fig. 1E), and the number of CPT-induced cells in mitotic phase arrest was comparable the number of untreated cells at the same stage (Fig. 1F). These results indicated that Mad2 is a key factor in CPT-induced mitotic phase arrest.

3.2. CPT-induced Mad2 upregulates cyclin B1 and Cdk1

Mad2 delays metaphase progression by associating with Cdc20 to inhibit APC activity, which prevents the degradation of securin/cyclin B1, as shown by the accumulation of cyclin B1 in mitotic phase arrest (Zeng et al., 2010). Western blot analysis showed that CPT induced significant increases in Cdk1 and cyclin B1 levels at 18 h (Fig. 2A). We also determined whether transient depletion of *Mad2* expression by siMad2 inhibits CPT-induced increases in Cdk1 and cyclin B1 levels. The CPT-induced increase in Cdk1 and cyclin B1 levels was markedly reduced in siMad2-transfected cells (Fig. 2B), which suggest that Cdk1 activity and cyclin B1 expression are enhanced by CPT-induced Mad2. Next, we measured whether transient knockdown of *Mad2* downregulates Cdk1 activity and intracellular cyclin B1 expression in response to CPT. Cdk1 activity was upregulated 6 h after treatment with CPT and reached maximum levels at 24 h (Fig. 2C). However, Cdk1 activity did not increase when siMad2-transfected cells were treated with CPT. We also examined the subcellular localization of cyclin B1, using immunofluorescence staining, to detect cyclin B1 upregulation in the presence or the absence of Mad2. Cyclin B1-GFP levels drastically increased upon treatment with CPT, when compared to the untreated control (Fig. 2D). However, the intensity of cyclin B1-GFP levels was strongly reduced upon transient knockdown of *Mad2*. These results indicate that CPT-induced Mad2 upregulates Cdk1 activity and cyclin B1 expression.

3.3. CPT positively activates Sp1 by inducing JNK phosphorylation, leading to Mad2-mediated mitotic arrest

Recent data suggested that the JNK signaling pathway controls mitotic phase to allow chromosomal instability induced by spindle checkpoint defects (Hirota et al., 2005). Therefore, we evaluated the role of JNK in CPT-induced mitotic arrest in LNCaP cells. Treatment with 2 μM CPT increased JNK phosphorylation in a time-dependent manner (Fig. 3A). JNK phosphorylation was clearly detected after 12 h and peaked at 18 h; however, total JNK level was not affected. A previous study showed that JNK induces phosphorylation and activation of several transcription factors, including Sp1, during mitotic phase (Chuang et al., 2008). Therefore, we analyzed the nuclear translocation and activity of Sp1. Western blot analysis showed that CPT caused a gradual disappearance of Sp1 from the cytosol and translocation of Sp1 to the nucleus (Supplementary Fig. 2A). Additionally, CPT enhanced the DNA-binding activity of Sp1 in a time-dependent manner (Supplementary Fig. 2B). To clarify the role of JNK in CPT-induced mitotic phase arrest, we used *JNK*-targeted siRNA (siJNK) to suppress JNK expression in LNCaP cells. Transfection of siJNK significantly decreased CPT-induced DNA-binding activity of Sp1, which confirmed that CPT-induced JNK phosphorylation activates Sp1 (Supplementary Fig. 2C). Furthermore, transfection of siJNK abrogated the CPT-induced increase in c-Jun phosphorylation, when compared to that in cells transfected with control siRNA (siCON) (Fig. 3B). Similarly, transient knockdown of *JNK* suppressed the CPT-induced upregulation of Mad2, Cdk1, and cyclin B1, suggesting that JNK phosphorylation contributes

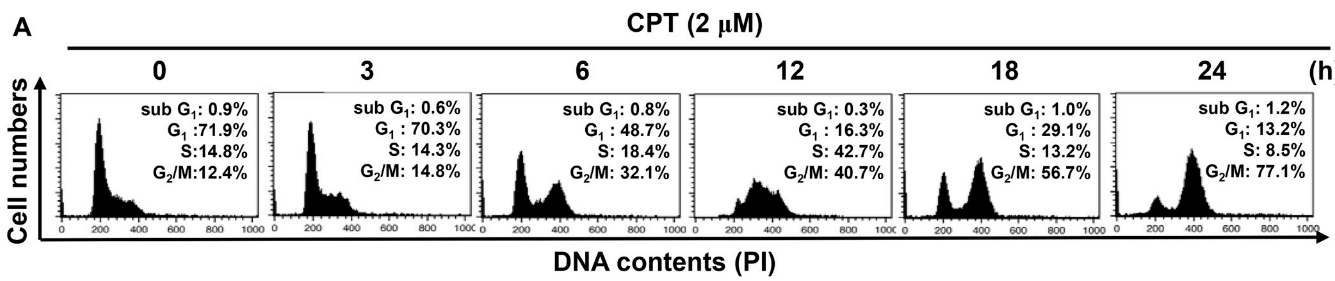

Phases \ Time (h)	CPT (2 μM) 0	3	6	12	18	24
Sub G_1	0.9±1.2%	0.6±0.9%	0.8±3.5%	0.3±1.1%	1.0±1.3%	1.2±2.1%
G_1	71.9±5.2%	70.3±1.9%	48.7±2.6%*	16.3±3.5%*	29.1±2.5%*	13.2±3.3%*
S	14.8±2.3%	14.3±3.8%	18.4±4.5%	42.7±4.2%*	13.2±3.5%	8.5±4.5%
G_2/M	12.4±3.5%	14.8±2.4%	32.1±3.5%*	40.7±5.1%*	56.7±2.8%*	77.1±3.9%*

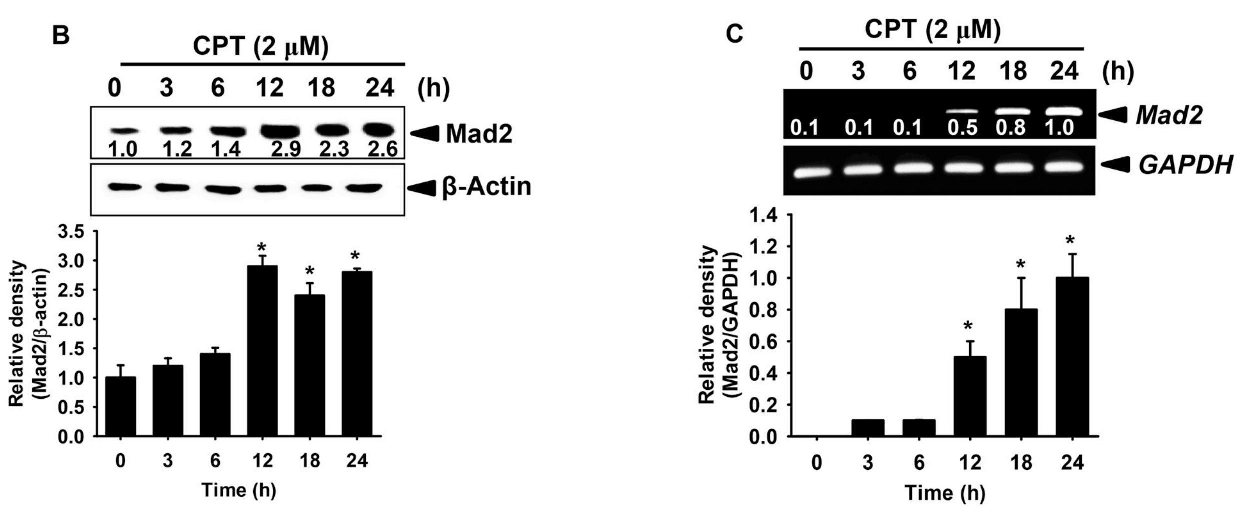

Fig. 1. Camptothecin (CPT)-induced Mad2 expression in LNCaP cells. LNCaP cells were seeded at 1×10^5 cells/ml and then treated with 2 μM CPT for the indicated times. (A) Cell cycle progression was analyzed by flow cytometry. (B) Total protein was subjected to 10% SDS-PAGE followed by western blot analysis with antibodies specific for Mad2. (C) In a parallel experiment, mRNA was harvested and RT-PCR was performed for *Mad2*. (D) Cell lysates were immunoprecipitated with anti-Cdc20 antibody and precipitated with protein-A/G agarose. Bound proteins were separated by gel electrophoresis and analyzed by western blot analysis with antibodies specific for Mad2. (E and F) Effect of Mad2 on CPT-induced mitotic arrest. After LNCaP cells were transfected with *Mad2*-targeted siRNA (siMad2) and control siRNA (siCON) for 48 h and then treated with CPT for additional 24 h, total protein was subjected to 10% SDS-PAGE followed by western blot analysis (E). Cell cycle distribution was analyzed using a flow cytometer (F). Statistical significance was determined by one-way ANOVA (*, $p < 0.05$ *vs*. 0 h and #, $p < 0.05$ *vs*. CPT-treated group transfected with siCON).

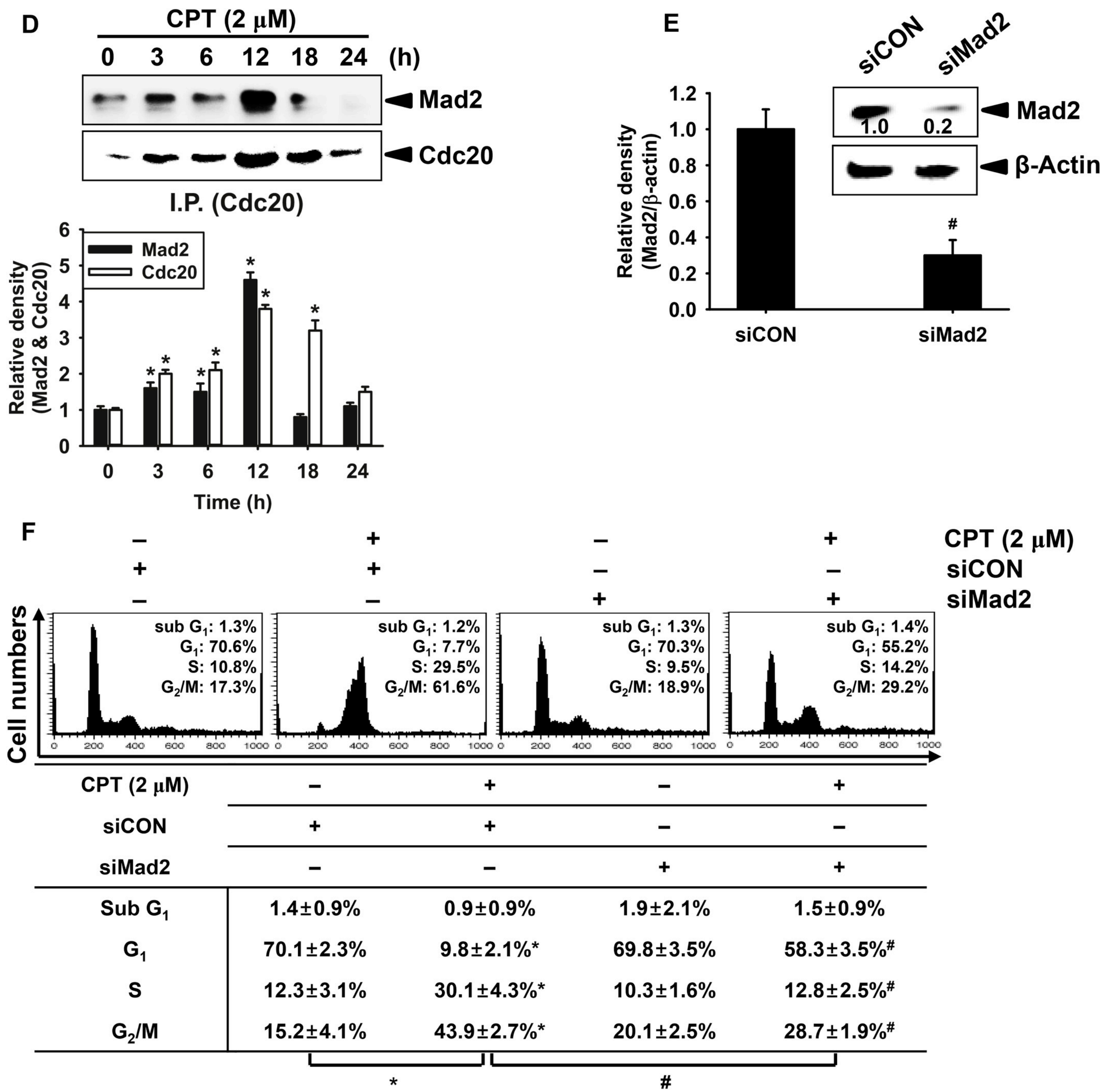

Fig. 1. (*continued*)

to CPT-induced mitotic phase arrest by inducing Mad2-mediated between cyclin B1 and Cdk1 expression. To determine whether CPT-induced JNK directly influences mitotic phase arrest, we analyzed cell cycle progression. Flow cytometric analysis showed that siJNK completely reversed CPT-induced mitotic phase arrest without inducing apparent apoptotic sub-G_1 phase (Fig. 3C). These data suggested that CPT-induced JNK is an important regulator of mitotic arrest by activating Mad2, resulting in Sp1 activation, which activates *Mad2*, *Cdk1*, and *cyclin B1*.

3.4. p21 promotes Mad2 expression in response to CPT

To determine the relation between increased p21 and CPT-induced mitotic phase arrest, we analyzed p21 expression and phosphorylation. CPT significantly induced p21 protein expression and phosphorylation (Fig. 4A). CPT also gradually promoted significant accumulation of *p21* mRNA (Fig. 4B). p21 is directly phosphorylated on Thr^{145} and Ser^{146} by the activating survival kinases, PI3K and Akt, and PTEN blocks Akt activation by suppressing PI3K. Lin et al., showed that transient knockdown of *PTEN* increased p21 stability, leading to the resistance to cisplatin-induced apoptosis that is associated with increased level of p21 (Lin et al., 2007). Therefore, we hypothesized that CPT regulates expression and phosphorylation of PTEN. As predicted, treatment with CPT decreased the levels of phosphorylated PTEN and total PTEN expression in a time-dependent manner (Fig. 4C). Next, we attempted to determine the precise role of p21 in CPT-induced mitotic phase arrest. Transient transfection of *p21* siRNA (sip21) significantly decreased the population of CPT-induced mitotic phase cells, but did not affect the population of sub-G_1 cells (Fig. 4D); however, cell cycle progression did not return to normal in cells transfected with sip21, suggesting that p21

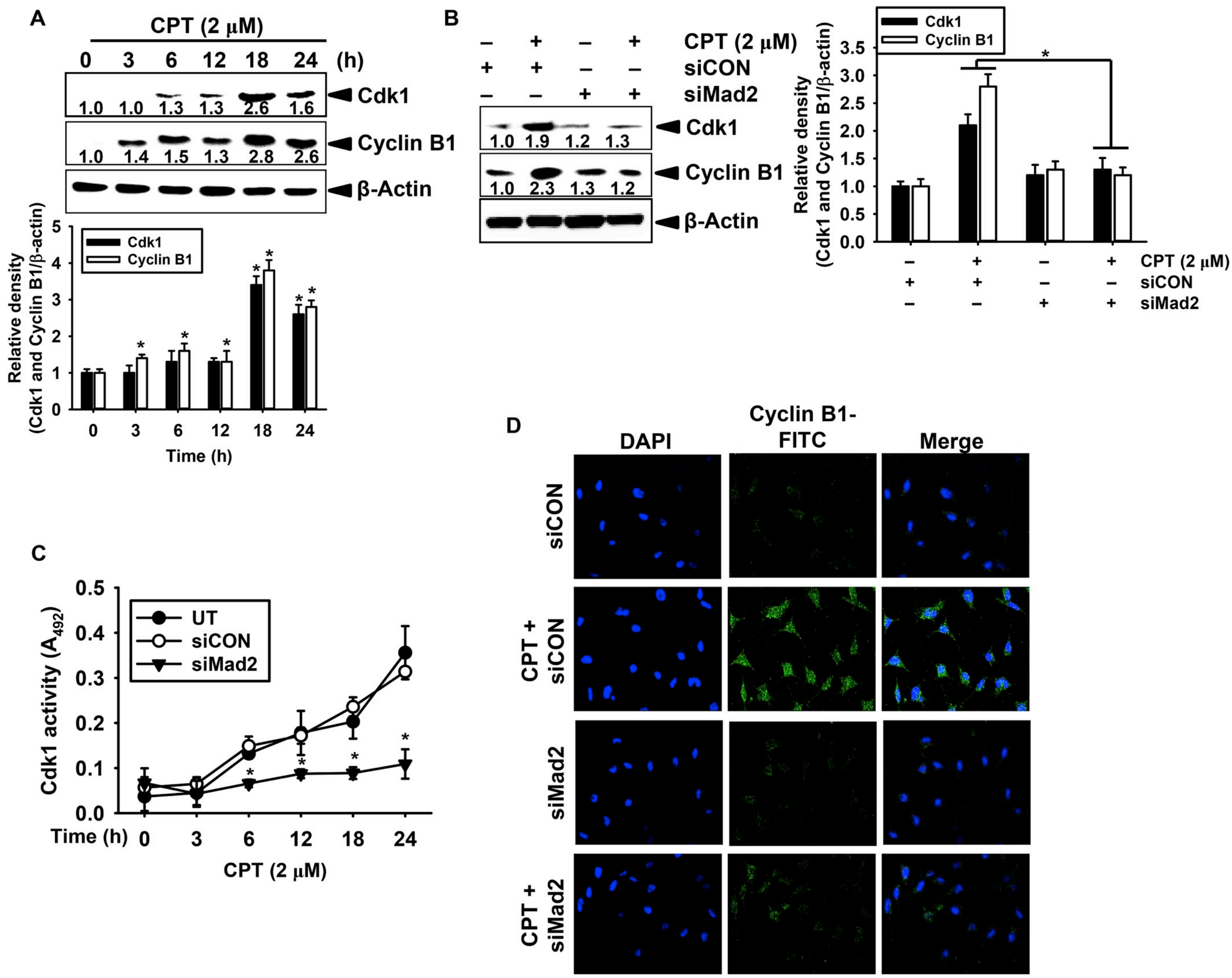

Fig. 2. Effect of camptothecin (CPT) on cyclin B1 and Cdk1. (A) LNCaP cells were seeded at 1×10^5 cells/ml and treated with 2 μM CPT for the indicated time points. Cell extracts were prepared for western blot analysis for Cdk1 and cyclin B1. (B) After LNCaP cells were transfected with *Mad2*-targeted siRNA (siMad2) and control siRNA (siCON) for 48 h, the cells were treated with 2 μM CPT for the indicated time points and then western blot analysis was performed with antibodies specific anti-Cdk1 and anti-cyclin B1. (C and D) LNCaP cells were seeded at 1×10^5 cells/ml and were treated with 2 μM CPT for the indicated times in the presence and absence of siMad2. Cdk1 activity was measured using an MESACUP Cdk1 kinase assay kit (C). In a parallel experiment, cyclin B1 level was analyzed by immunofluorescence staining. LNCaP cells were fixed, permeabilized, and stained with a antibody against cyclin B1. The antibody was detected using an anti-rabbit secondary antibody, conjugated to FITC, under confocal microscopy (D). Statistical significance was determined by one-way ANOVA [*, $p < 0.05$ *vs*. each control at 0 h (A and C)] and Student's *t*-test [*, $p < 0.05$ *vs*. CPT-treated group transfected with siCON (B)].

is partially associated with CPT-induced mitotic phase arrest. Nevertheless, transient knockdown of p21 decreased CPT-induced Mad2 and cyclin B1 levels (Fig. 4E), as well as Cdk1 activity (Fig. 4F), which suggested that p21 is an upstream regulator of Mad2-mediated cyclin B1 and Cdk1 expression. Finally, a total Cdk inhibitor (CdkI) completely restored CPT-induced mitotic phase arrest to normal untreated cell cycle progression (Fig. 4G). These data indicated that p21 is associated with CPT-induced mitotic phase arrest via Mad2-mediated cyclin B1 and Cdk1 expression.

3.5. CPT stimulates Mad2 expression by inducing tubulin polymerization

To determine whether CPT activates Mad2 via tubulin or actin dysfunction in human LNCaP cells, we treated the cells with 2 μM CPT. Treatment with CPT increased the size of nuclear structure and enhanced the intensity of α-tubulin staining, as measured by laser scanning confocal microscopy (Fig. 5A, *top*); the treatment also increased cell size (Fig. 5A, *bottom*), when compared to that of untreated cells. Flow cytometric analysis also showed that treatment with CPT caused a significant increase of forward scatter (FSC), which indicates cell size, and side scatter (SSC), which indicates cell granularity (Fig. 5B). These results indicated that CPT-induced mitotic phase arrest results in cell division followed by increased cell size and granularity. Additionally, we found that long-term, 48 h treatment with CPT caused an increase in the number of cells in mitotic phase arrest, resulting in an endoreduplicated cell population (> 4N), which blocked cell division (Fig. 5C); however, the long-term treatment for 48 h did not increased the cell population of sub-G_1 phase. Moreover, to identify the CPT target responsible for CPT-mediated mitotic phase arrest and endoreduplication, we determined whether CPT regulates polymerization or depolymerization of either tubulin or actin, which are the main drivers of cytoskeletal dynamics during cell division. Treatment with CPT induced significantly more tubulin polymerization at 3 min than that in the untreated control, similar to the levels of tubulin polymerization in paclitaxel-treated positive controls, which indicated that CPT enhances tubulin polymerization (Fig. 5D). However, treatment

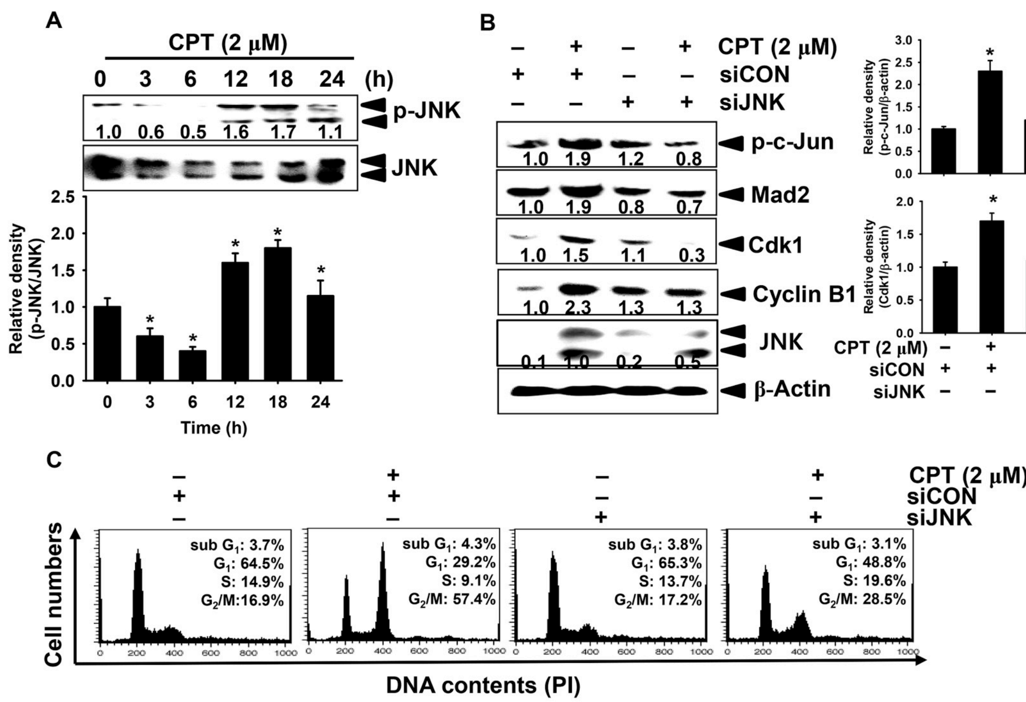

CPT (2 μM)	−	+	−	+
siCON	+	+	−	−
siJNK	−	−	+	+
Sub G_1	3.7±1.3%	4.5±2.1%	3.5±2.9%	3.3±1.8%
G_1	66.3±4.2%	28.3±3.5%*	64.9±4.8%	49.8±3.5%#
S	16.9±2.3%	10.6±5.1%	14.2±2.8%	18.9±2.3%
G_2/M	18.2±3.1%	55.9±5.9%*	18.9±3.4%	26.9±3.6%#

* (columns 1 vs 2); # (columns 2 vs 4)

Fig. 3. Effect of camptothecin (CPT) on JNK-mediated Sp1 activation. (A) LNCaP cells were seeded at 1×10^5 cells/ml and treated with 2 μM CPT for the indicated time points. Equal amounts of cell lysate were resolved on SDS-polyacrylamide gels, transferred to nitrocellulose membranes, and probed with antibody against p-JNK and JNK. (B) After LNCaP cells were transfected with *JNK*-targeted siRNA (siJNK) and control siRNA (siCON) for 48 h, the cells were treated with 2 μM CPT for 24 h. Cell lysates were isolated and western blot analysis was performed with antibodies against p-c-Jun, Mad2, Cdk1, JNK, and cyclin B1. (C) In a parallel experiment, cell cycle progression was measured by DNA content (PI staining) 24 h after treatment with CPT. Statistical significance was determined by and one-way ANOVA [*, $p < 0.05$ *vs.* each control at 0 h (A)] and Student's *t*-test [*, $p < 0.05$ *vs.* each control at 0 h and $^\#$, $p < 0.05$ *vs.* CPT-treated group transfected with siCON (B and C)].

with nocodazole decreased tubulin polymerization. As shown in western blot analysis, treatment with CPT increased polymeric α-tubulin levels similar to that caused by treatment with paclitaxel (Fig. 5E). In a parallel experiment, CPT-induced Mad2 expression was detected, which suggested that CPT-induced tubulin polymerization is a hallmark for blocking cell division through activation of the mitotic checkpoint protein, Mad2. Phalloidin-FITC staining showed that neither actin polymerization nor actin depolymerization is a target of CPT-mediated mitotic phase arrest (Fig. 5F). Taken together, these data indicated that CPT-induced tubulin polymerization blocks cell division as a result of mitotic phase arrest and endoreduplication.

3.6. Autophagy formation enhances CPT-induced mitotic phase arrest

Recent studies showed that accumulation of several procaspases in mitotic phase blocks apoptosis (Allan and Clarke, 2007; Matthess et al., 2010). Therefore, we examined whether CPT enhances mitotic phase arrest in LNCaP cells by blocking apoptosis through the accumulation of procaspases. Western blot analysis confirmed that treatment with CPT caused a time-dependent increase in procaspase-9 and procaspase-8 expression (Fig. 6A). To verify that caspase-9 and autophagy regulate apoptosis in CPT-induced mitotic phase arrest, we examined cell cycle progression. CPT-induced mitotic phase arrest was decreased in the presence of z-LEHD-FMK and 3 MA, and treatment with these inhibitors did not induce apoptosis; but delayed the mitotic phase arrest by staying at G_1 phase, suggesting that procaspase-9 accumulation and autophagy formation delays CPT-induced cell cycle progression at G_1 phase. However, transfection with siMad2 enhanced apoptotic sub-G_1 phase from the z-LEHD-FMK- and 3 MA-induced mitotic arrest (Fig. 6B). Finally, western blot analysis showed that transfection with siMad2 downregulated procaspase-9 and procaspase-8, and upregulated Bax in response to treatment with CPT, together with z-LEHD-FMK or 3 MA (Fig. 6C). Intriguingly, these data indicated that inhibition of autophagy and caspase-9 decreased CPT-induced mitotic phase arrest and depletion of Mad2 increased CPT-mediated apoptosis in the presence of z-LEHD-FMK and 3 MA.

4. Discussion

A previous study showed that CPT is a novel anticancer drug with immunomodulatory, anti-cancerous, and anti-proliferative properties (Zare-Mirakabadi et al., 2012), which are caused, in part, by its strong

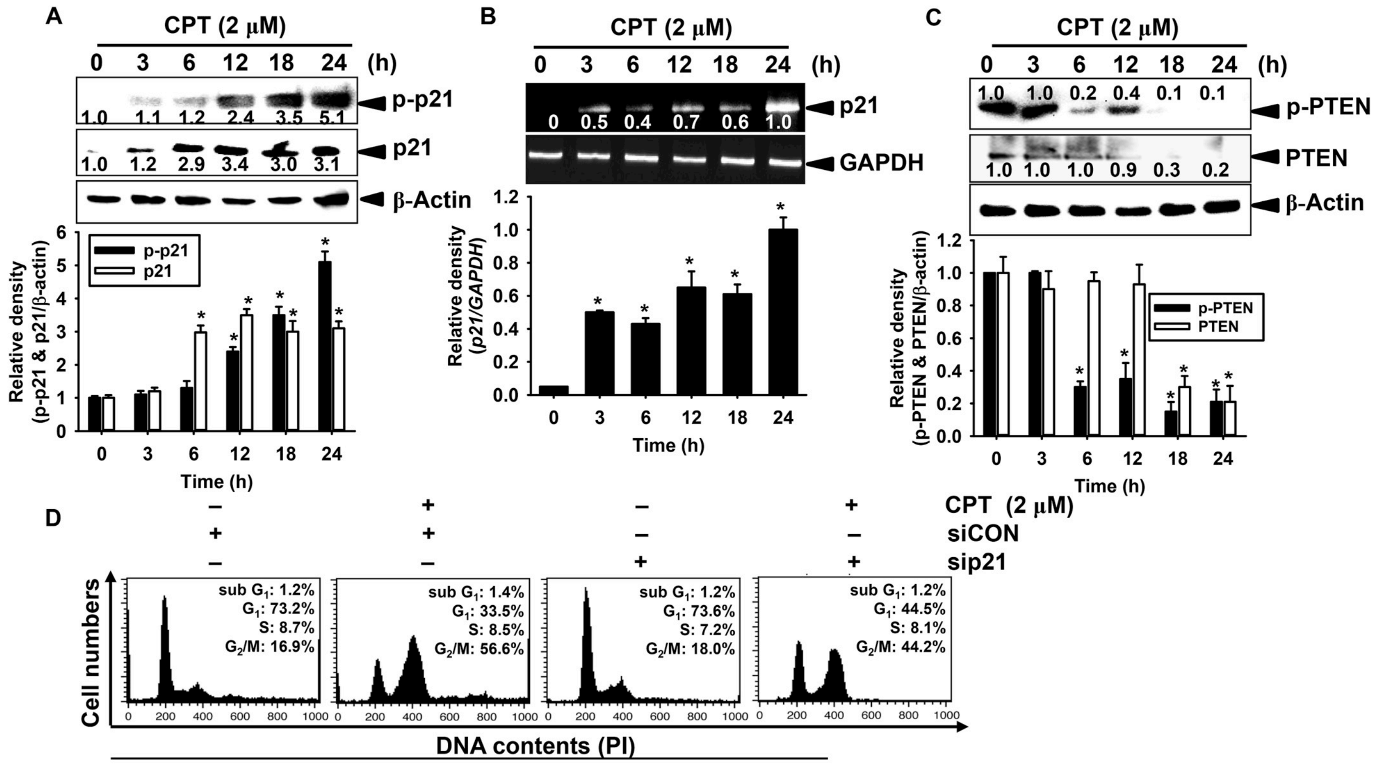

CPT (2 μM)	−	+	−	+
siCON	+	+	−	−
sip21	−	−	+	+
Sub G_1	2.1±1.7%	2.9±1.1%	1.6±1.3%	1.9±1.1%
G_1	70.3±2.9%	32.1±3.5%*	73.1±5.2%	46.3±6.3%#
S	10.2±3.4%	9.4±3.6%	8.6±3.8%	8.9±3.5%
G_2/M	17.1±2.5%	56.7±4.5%*	17.5±2.4%	42.5±4.2%#

Fig. 4. Effect of camptothecin (CPT) on p21 in LNCaP cells. LNCaP cells were treated with 2 μM CPT for the indicated time points. Total protein was subjected to 10% SDS-PAGE followed by western blot analysis with antibodies specific for phosphorylated forms of p21(A) and PTEN (C). β-Actin was used as an internal control. (B) Total RNA was isolated and RT-PCR analysis for *p21* was performed. *GAPDH* was used as a loading control. (D and E) LNCaP cells were transiently transfected with *p21*-targeted siRNA (sip21) and control siRNA (siCON) for 48 h and then treated with 2 μM CPT for additional 24 h. (D) DNA content was analyzed using a flow cytometer. (E) Whole-cell protein lysates were prepared for detection of the indicated proteins by western blot analysis. (F and G) LNCaP cells were pretreated with a total Cdk inhibitor (CdkI) 2 h before transfection of sip21 for 24 h and then CPT was treated for 24 h Cdk1 activity was measured using an MESACUP Cdk1 kinase assay kit (F). DNA content was analyzed using a flow cytometer (G). Statistical significance was determined by and one-way ANOVA [*, $p < 0.05$ *vs.* each control at 0 h (A, B, and C)] and Student's *t*-test [*, $p < 0.05$ *vs.* each control at 0 h and #, $p < 0.05$ *vs.* CPT-treated group transfected with siCON (D, E, F, and G)].

inhibition of the DNA-replicating enzyme, topoisomerase I (Kim et al., 2015). We previously demonstrated that CPT inhibited cancer cell invasion by inhibiting expression of matrix metalloprotease-9 (MMP-9) and vascular endothelial growth factor (VEGF), via nuclear factor erythroid-derived 2-like 2 (Nrf2)-mediated heamoxygenase-1 (HO-1) (Jayasooriya et al., 2015). We also showed that CPT sensitized cancer cells to TNF-α-related apoptosis inducing ligand (TRAIL)-induced apoptosis (Jayasooriya et al., 2014). Additionally, studies have determined that CPT-induced cell cycle arrest occurs at different stages in various cell types (Park et al., 1997; Shao et al., 1997). Recently, Kim et al. (2015) reported that a synthetic, water-soluble CPT derivative, CKD-602, induced G_2/M phase arrest in oral squamous cancer cells. Nevertheless, the basic mechanism of CPT-induced cell cycle arrest has not been elucidated to date. CPT is a promising therapeutic for the treatment of cancers because it specifically targets topoisomerase I, which is highly activated in cancer cells; however, CPT has not been used in clinical trials because of its low solubility and severe side effects, such as diarrhea and hemorrhagic cystitis. Despite the adverse effect of CPT, because of its high specificity in cancer cells, many scientists seek to identify CPT derivatives. In this respect, continuing studies on the molecular mechanism of CPT might provide basic information about the molecular actions of CPT derivatives, since CPT derivatives would have anti-cancer effects similar to those of CPT. In the current study, we first determined that the molecular mechanism underlying CPT-induced mitotic phase arrest acted by inducing Mad2, resulting in upregulation of Cdk1 and cyclin B1 expression. Furthermore, CPT-induced Mad2 expression required JNK activation, which activates the transcription factor Sp1. Additionally, we found that CPT-induced accumulation of caspase-9 and autophagy results in Mad2-induced mitotic phase arrest by blocking apoptosis (Fig. 7).

SACs consistently monitor the integrity of spindle kinetochore attachment during prometaphase and metaphase to establish bipolar attachments (Gregan et al., 2011). Mad2, BubR1, and other checkpoint components form an inhibitory ternary complex with E3 ligase, APC/C, and Cdc20. Once sister kinetochores correctly attach to bipolar regions during metaphase, SACs are disabled and APC/Cdc20-meadiated

E

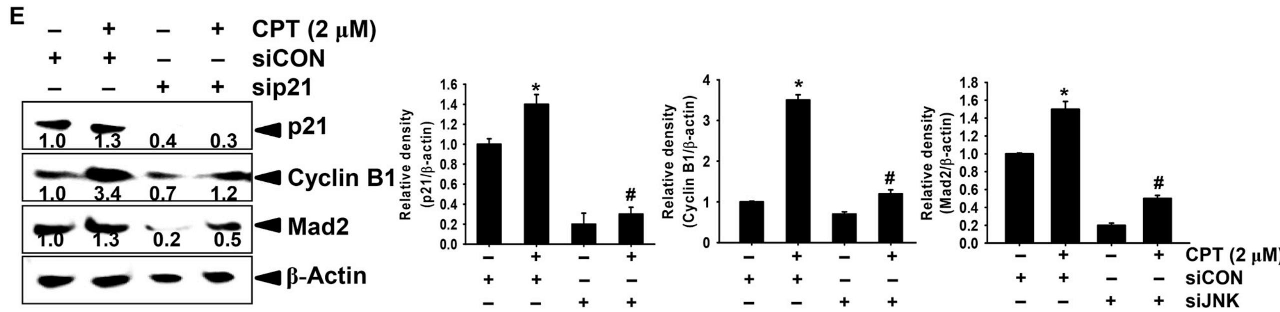

F

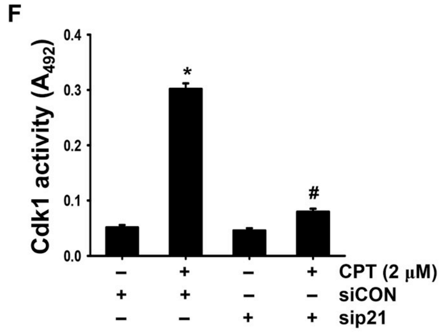

G

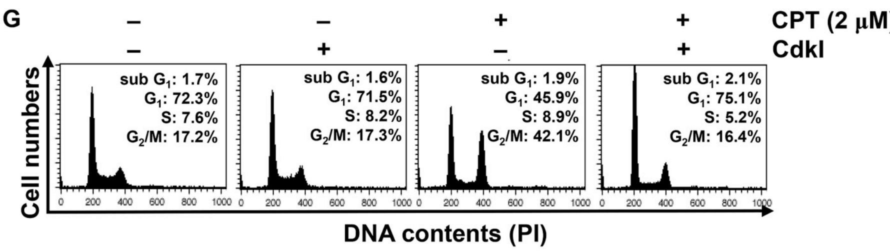

CPT (2 μM)	–	–	+	+
CdkI	–	+	–	+
Sub G_1	2.1±1.1%	2.1±1.8%	1.7±1.1%	3.2±2.7%
G_1	70.3±4.9%	69.8±3.2%	43.2±5.1%*	74.3±4.8%#
S	8.3±2.9%	9.5±5.7%	7.8±2.1%	7.1±2.5%
G_2/M	16.9±3.8%	17.8±3.8%	43.6±4.8%*	18.2±4.1%#

* #

Fig. 4. (*continued*)

ubiquitination of securin and cyclin B are required for the onset of anaphase (Foster and Morgan, 2012); however, when sister metaphase chromosomes are improperly attached to kinetochores, SACs, such as Mad2, are activated to delay cell cycle progression from metaphase to anaphase (Allan and Clarke, 2007). In the present study, we showed that Mad2 is upregulated at the transcriptional and translational levels in response to CPT. This finding indicated that CPT deregulates kinetochore attachment by inducing Mad2. We also found that CPT increased H3 phosphorylation, a mitotic phase marker, suggesting that CPT induces mitotic phase arrest. Additionally, transient knockdown of *Mad2* completely prevented CPT-induced mitotic phase arrest. Taken together, we concluded that CPT caused the improper connection of microtubules to the kinetochores of sister chromosomes, resulting in the activation of SACs and consequently delaying or halting prometaphase or metaphase. In this study, we also found that depletion of *Mad2* abrogated CPT-induced enhancement of cyclin B1 and Cdk1 expression, suggesting that Mad2 mediates the upregulation of cyclin B1 and Cdk1. Transition from G_2 phase to mitotic phase is triggered by activation of the cyclin B1/Cdk1 complex, which is sustained from prometaphase to metaphase and is completely destroyed in anaphase; in contrast, low activity of the cyclin B1/Cdk1 complex arrests cell cycle progression in S phase (Castedo et al., 2002). Here, we demonstrated that silencing of *Mad2* significantly reduced CPT-induced mitotic phase accumulation without apoptotic sub-G_1 phase. Taken together, our data indicate that treatment with CPT causes prometaphase or metaphase arrest, without causing apoptosis, by inducing the Mad2-mediated cyclin B1/Cdk1 expression, and that this effect result from unstable binding of microtubules to kinetochores of sister chromosomes. Nevertheless, our data found that in vitro assay, CPT significantly upregulates tubulin polymerization, which suggests that CPT may directly bind to tubulin polymer and block its dissociation.

A study recently reported that JNK induced prometaphase and metaphase arrest by inducing JNK-mediated cyclin B1 and Cdk1 expression through the phosphorylation and inhibition of Cdc25C (Ribas et al., 2012). Additionally, JNK stabilized Sp1 via phosphorylation at Thr^{278} ^{and} Thr^{739}, leading to the activation of *p21*, which has six Sp1 binding sites in the core promoter region (Chuang et al., 2008; Gartel et al., 2000). Our earlier study showing that the JNK inhibitor, SP600125, inhibited the increase in cellular p21 levels demonstrates the importance of JNK in p21 expression (Moon et al., 2011). In the present study, CPT-induced Mad2 is required for JNK activation, which in turn phosphorylates the transcription factor, Sp1, thereby increasing Sp1 DNA-binding activity. Nevertheless, further experiments are needed to identify other Mad2-regulating transcription factors, because many transcription factors, such as AP1, ATF-2, and NF-κB, directly bind to the *Mad2* promoter region and because *Mad2* is partially regulated by p53, Braca1, and Tax (Idikio, 2006). We also found that knockdown of *p21* restored CPT-induced mitotic phase arrest. These data indicate that the JNK/Sp1/p21 pathway is involved in CPT-induced mitotic phase arrest. p21 is a well-known Cdk inhibitor that directly binds and inhibits the cyclin B1-Cdk1 complex during the transition from G_2 to mitotic phase, and functions in G_2/mitotic phase arrest (Gire and Dulic, 2015); however, in the present study, we found that p21 and the cyclin B1-Cdk1 complex are simultaneously upregulated in response to CPT, suggesting that CPT regulates mitotic phase arrest, not the transition from G_2 to mitotic phase. In agreement with our data, previous studies demonstrated that the treatment of cancer cells with microtubule inhibitors, such as vinblastine, paclitaxel, and nocodazole, causes upregulation of Mad2 and the cyclin B1 and Cdk1 complex (Abbas and Dutta, 2009; Choi and Zhu, 2012; Xiao et al., 2003); however, there was no explanation for the simultaneous upregulation of p21. Charrier-Savournin et al., clearly demonstrated that p21 tightly sequesters the cyclin B1 and Cdk1 complex (Charrier-Savournin et al., 2004), thereby inactivating the complex and, consequently,

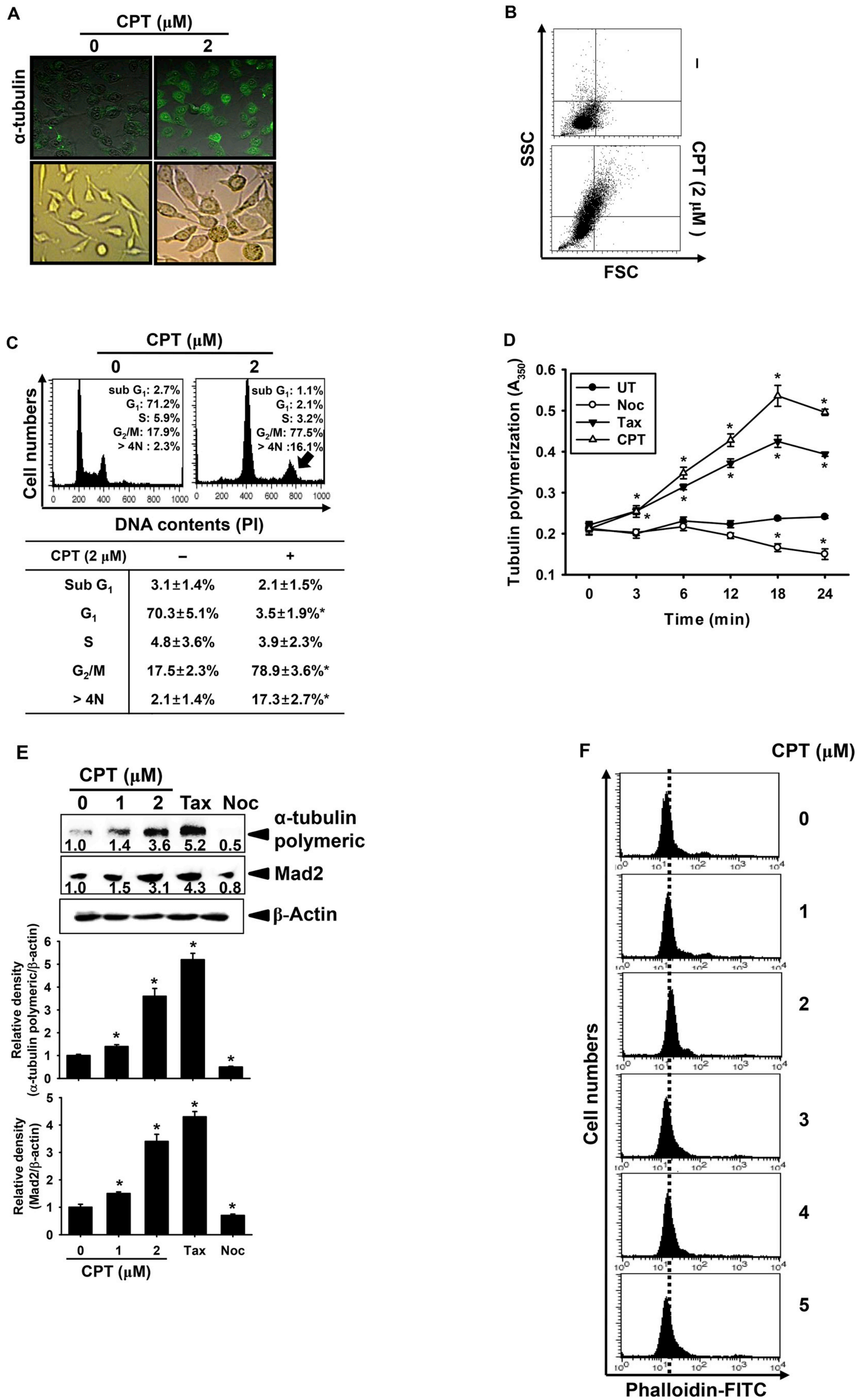

CPT (2 μM)	–	+
Sub G_1	3.1±1.4%	2.1±1.5%
G_1	70.3±5.1%	3.5±1.9%*
S	4.8±3.6%	3.9±2.3%
G_2/M	17.5±2.3%	78.9±3.6%*
> 4N	2.1±1.4%	17.3±2.7%*

(caption on next page)

Fig. 5. Effect of camptothecin (CPT) on tubulin polymerization. LNCaP cells were seeded at 1×10^5 cells/ml and treated with 2 μM CPT for 48 h. (A) LNCaP cells were stained with a antibody against tubulin and analyzed by fluorescence microscopy (*top*). Cell morphology was examined under a light microscopy (*bottom*). (B) LNCaP cell size (FSC) and intracellular granules (SSC) were detected by flow cytometric analysis 48 h after treatment with CPT. (C) LNCaP cells were treated with 2 μM CPT for 48 h. The cells were stained with propidium iodine and analyzed by flow cytometry. (D) Effects of CPT on in vitro microtubulin polymerization. Microtubule associated protein-rich tubulin (1 mg/ml) was incubated at 37 °C for 0–24 min after treatment with 2 μM CPT, 3 μM nocodazole (Noc), and 3 μM paclitaxel (Tax). (E) LNCaP cells were treated with CPT (1 μM and 2 μM), 3 μM Noc, and 3 μM Tax for 48 h and then whole-cell protein lysates were prepared for detection of the Mad2 and polymeric tubulin by western blot analysis. β-Actin was used as the internal control. (F) LNCaP cells were treated with CPT for the indicated concentrations for 48 h. The cells were stained with phalloidin-FITC and then analyzed using flow cytometry. Statistical significance was determined by one-way ANOVA (*, $p < 0.05$ *vs.* each control at 0 h).

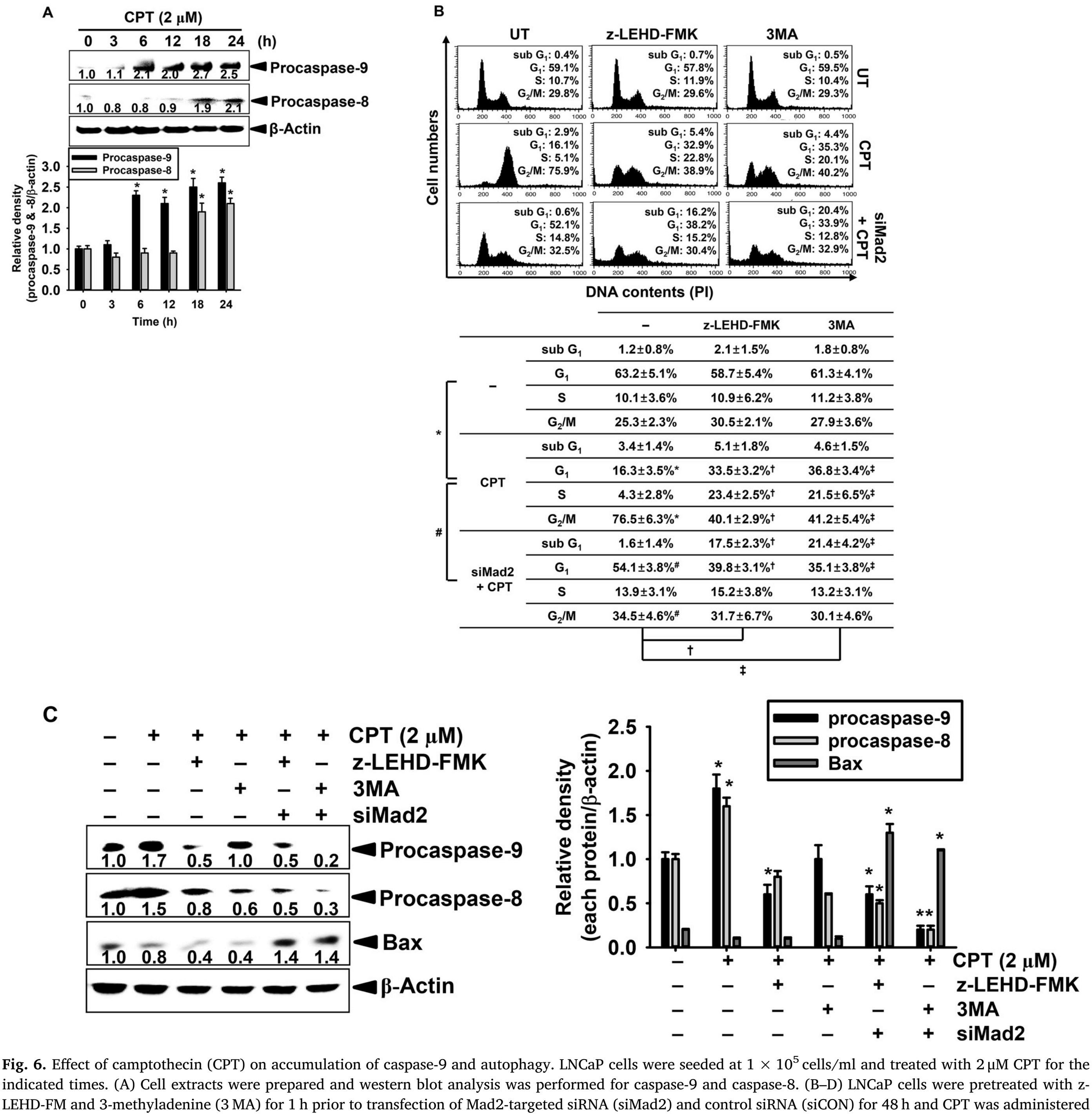

		–	z-LEHD-FMK	3MA
–	sub G_1	1.2±0.8%	2.1±1.5%	1.8±0.8%
	G_1	63.2±5.1%	58.7±5.4%	61.3±4.1%
	S	10.1±3.6%	10.9±6.2%	11.2±3.8%
	G_2/M	25.3±2.3%	30.5±2.1%	27.9±3.6%
CPT	sub G_1	3.4±1.4%	5.1±1.8%	4.6±1.5%
	G_1	16.3±3.5%*	33.5±3.2%†	36.8±3.4%‡
	S	4.3±2.8%	23.4±2.5%†	21.5±6.5%‡
	G_2/M	76.5±6.3%*	40.1±2.9%†	41.2±5.4%‡
siMad2 + CPT	sub G_1	1.6±1.4%	17.5±2.3%†	21.4±4.2%‡
	G_1	54.1±3.8%#	39.8±3.1%†	35.1±3.8%‡
	S	13.9±3.1%	15.2±3.8%	13.2±3.1%
	G_2/M	34.5±4.6%#	31.7±6.7%	30.1±4.6%

Fig. 6. Effect of camptothecin (CPT) on accumulation of caspase-9 and autophagy. LNCaP cells were seeded at 1×10^5 cells/ml and treated with 2 μM CPT for the indicated times. (A) Cell extracts were prepared and western blot analysis was performed for caspase-9 and caspase-8. (B–D) LNCaP cells were pretreated with z-LEHD-FM and 3-methyladenine (3 MA) for 1 h prior to transfection of Mad2-targeted siRNA (siMad2) and control siRNA (siCON) for 48 h and CPT was administered for 24 h. (B) DNA content was analyzed by flow cytometry. (C) In a parallel experiment, western blot analysis was performed for caspase-9, caspase-8, and Bax. Statistical significance was determined by and one-way ANOVA [*, $p < 0.05$ *vs.* each control at 0 h (A and D)] and Student's *t*-test [*, $p < 0.05$ *vs.* CTP-treated group (C), and [*, $p < 0.05$ *vs.* untreated control, $^\#$, $p < 0.05$ *vs.* CPT-treated group, †, $p < 0.05$ *vs.* each inhibitor-untreated group, and ‡, $p < 0.05$ *vs.* each inhibitor-untreated group (C)].

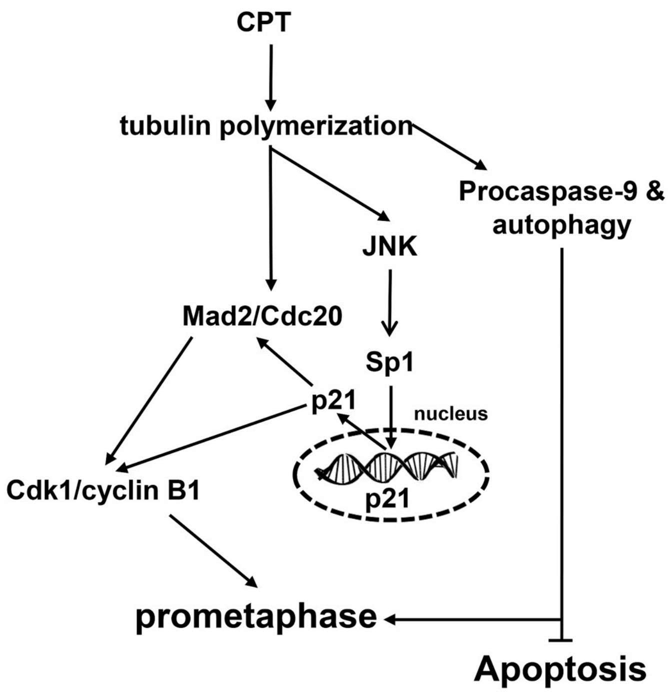

Fig. 7. Schematic model for camptothecin (CPT)-induced mitotic arrest. CPT directly binds to the topoisomerase I-DNA complex, resulting in a ternary complex and irreversibly stabilizing it. This model suggests that, unlike other drugs that directly target tubulin, such as nocodazole and paclitaxel, CPT indirectly targets tubulin polymerization to affect chromosome instability. During CPT-induced chromosome instability, kinetochores lose equal microtubule tension by tubulin polymerization, leading to engagement of Mad2, which prevents cell cycle progression from prometaphase to metaphase and anaphase by inducing cyclin B1 and Cdk1 complex. Moreover, c-Jun-N-terminal kinase (JNK) partially stimulates Sp1-mediated p21 in Mad2-induced mitotic arrest in response to CPT. Additionally, autophagy formation and accumulation of procaspase-9 are required for the rapid increase of CPT-induced mitotic arrest. Following a prolonged prometaphase arrest, the CPT-treated cells are expected to undergo endoreduplication before apoptosis.

maintaining G_2 phase arrest (Dulic et al., 1998). Interestingly, Lindgvist et al. (2007) proposed that mitotic cyclin B1-Cdk1 activity gradually increases after mitotic phase entry, and that this activity is sustained in metaphase, allowing efficient mitotic progression and the initiation of mitotic exit. Moreover, microtubule inhibitors dramatically stabilized p21 in the mitotic phase, mainly by sustaining p21 in the cytosol, rather than the nucleus, thereby assisting the cell survival signal (Kreis et al., 2015). Although additional experiments are needed to determine whether p21 is in the cytosol or the nucleus during mitotic phase arrest, CPT-induced p21 might act in the cytosol to trigger the cell survival signal, and free, CPT-induced cyclin B1-Cdk1 complexes may monitor mitotic phase progression.

Yagdi Efe et al. (2017) recently suggested that cell cycle progression and apoptosis may be closely linked, and thus, cell cycle checkpoint molecules are prerequisites for apoptosis; in particular, during mitotic phase arrest, apoptosis appears to be restrained. We previously found that apoptosis does not occur in response to CPT treatment by activating endoplasmic reticulum stress-mediated autophagy (Jayasooriya et al., 2018), thus promoting endoreduplication. Surprisingly, the new function for the cyclin B1-Cdk1 complex during mitosis suggested that key regulators that induce apoptosis, such as caspase-8 and caspase-9, are phosphorylated, leading to their inactivation (Parrish et al., 2013). In mitotic cells, procaspase-8 is phosphorylated by Cdk1/cyclin B1, on Ser^{387}, which protects mitotic cells from extrinsic death stimuli (Matthess et al., 2010). Caspase-9 is also phosphorylated in mitotic cells by a Cdk1/cyclin B1, on Thr^{125}. This phosphorylation induces mitotic arrest by microtubule dysfunction, and an unphosphorylatable mutant is sensitive to apoptosis (Allan and Clarke, 2007). In the present study, CPT induced the accumulation of procaspases-8 and procaspase-9 during mitotic arrest; unexpectedly, a caspase-9 inhibitor only decreased CPT-induced mitotic arrest through an unclear mechanism. An autophagy inhibitor, 3 MA, showed the same molecular pattern as the caspase-9 inhibitor, z-LEHD-FMK, which suggests that accumulation of procaspase-9 and autophagy protects apoptosis, leading to CPT-induced mitotic arrest. Moreover, under condition of transient knockdown of *Mad2*, z-LEHD-FMK and 3 MA significantly enhanced apoptosis while restoring cell cycle progression from CPT-induced mitotic arrest, indicating that depletion of Mad2 induced apoptosis during the inhibition of capase-9 and autophagy in response to CPT. Taken together, our data indicate that CPT induces Mad2-mediated autophagy and the accumulation of procaspase-9 and thus enhances mitotic phase arrest by blocking apoptosis.

In summary, our findings indicate that unstable microtubule dynamics, in response to CPT treatment, lead to prometaphase or metaphase arrest by inducing Mad2-mediated formation of cyclin B1 and Cdk1 complex via the JNK/Sp1/p21 pathway. Moreover, the CPT-induced delay of apoptosis was also related to autophagy and the accumulation of procaspase-9. These novel biological properties of CPT may facilitate understanding of the molecular action of topoisomerase I-mediated tubulin targeting drugs.

Conflicts of interest

The authors have declared that no competing interest exists.

Acknowledgment

The research was supported by the Program of National Research Foundation of Korea through the Ministry of Education.

Appendix A. Supplementary data

Supplementary data to this article can be found online at https://doi.org/10.1016/j.fct.2019.03.026.

Transparency document

Transparency document related to this article can be found online at https://doi.org/10.1016/j.fct.2019.03.026.

References

Abbas, T., Dutta, A., 2009. p21 in cancer: intricate networks and multiple activities. Nat. Rev. Canc. 9, 400–414.
Allan, L.A., Clarke, P.R., 2007. Phosphorylation of caspase-9 by CDK1/cyclin B1 protects mitotic cells against apoptosis. Mol. Cell. 26, 301–310.
Castedo, M., Perfettini, J.L., Roumier, T., Kroemer, G., 2002. Cyclin-dependent kinase-1: linking apoptosis to cell cycle and mitotic catastrophe. Cell Death Differ. 9, 1287–1293.
Chadebech, P., Truchet, I., Brichese, L., Valette, A., 2000. Up-regulation of cdc2 protein during paclitaxel-induced apoptosis. Int. J. Cancer 87, 779–786.
Charrier-Savournin, F.B., Chateau, M.T., Gire, V., Sedivy, J., Piette, J., Dulic, V., 2004. p21-Mediated nuclear retention of cyclin B1-Cdk1 in response to genotoxic stress. Mol. Biol. Cell 15, 3965–3976.
Choi, H.J., Fukui, M., Zhu, B.T., 2011. Role of cyclin B1/Cdc2 up-regulation in the development of mitotic prometaphase arrest in human breast cancer cells treated with nocodazole. PLoS One 6 e24312.
Choi, H.J., Zhu, B.T., 2012. Critical role of cyclin B1/Cdc2 up-regulation in the induction of mitotic prometaphase arrest in human breast cancer cells treated with 2-methoxyestradiol. Biochim. Biophys. Acta 1823, 1306–1315.
Chuang, J.Y., Wang, Y.T., Yeh, S.H., Liu, Y.W., Chang, W.C., Hung, J.J., 2008. Phosphorylation by c-Jun NH_2-terminal kinase 1 regulates the stability of transcription factor Sp1 during mitosis. Mol. Biol. Cell 19, 1139–1151.
Dash, B.C., El-Deiry, W.S., 2005. Phosphorylation of p21 in G_2/M promotes cyclin B-Cdc2 kinase activity. Mol. Cell Biol. 25, 3364–3387.
Dulic, V., Stein, G.H., Far, D.F., Reed, S.I., 1998. Nuclear accumulation of $p21^{Cip1}$ at the onset of mitosis: a role at the G_2/M-phase transition. Mol. Cell Biol. 18, 546–557.

Field, J.J., Kanakkanthara, A., Miller, J.H., 2014. Microtubule-targeting agents are clinically successful due to both mitotic and interphase impairment of microtubule function. Bioorg. Med. Chem. 22, 5050–5059.

Foster, S.A., Morgan, D.O., 2012. The APC/C subunit Mnd2/Apc15 promotes Cdc20 autoubiquitination and spindle assembly checkpoint inactivation. Mol. Cell. 47, 921–932.

Gartel, A.L., Goufman, E., Najmabadi, F., Tyner, A.L., 2000. Sp1 and Sp3 activate p21 (WAF1/CIP1) gene transcription in the Caco-2 colon adenocarcinoma cell line. Oncogene 19, 5182–5188.

Ge, S., Skaar, J.R., Pagano, M., 2009. APC/C- and Mad2-mediated degradation of Cdc20 during spindle checkpoint activation. Cell Cycle 8, 167–171.

Gire, V., Dulic, V., 2015. Senescence from G_2 arrest, revisited. Cell Cycle 14, 297–304.

Gregan, J., Polakova, S., Zhang, L., Tolic-Norrelykke, I.M., Cimini, D., 2011. Merotelic kinetochore attachment: causes and effects. Trends Cell Biol. 21, 374–381.

Hirota, T., Lipp, J.J., Toh, B.H., Peters, J.M., 2005. Histone H3 serine 10 phosphorylation by Aurora B causes HP1 dissociation from heterochromatin. Nature 438, 1176–1180.

Idikio, H.A., 2006. Spindle checkpoint protein hMad2 and histone H3 phosphoserine 10 mitosis marker in pediatric solid tumors. Anticancer Res. 26, 4687–4694.

Jang, S.H., Kim, A.R., Park, N.H., Park, J.W., Han, I.S., 2016. DRG2 regulates G_2/M progression via the cyclin B1-Cdk1 complex. Mol. Cell 39, 699–704.

Jayasooriya, R., Dilshara, M.G., Karunarathne, W., Molagoda, I.M.N., Choi, Y.H., Kim, G.Y., 2018. Camptothecin enhances c-Myc-mediated endoplasmic reticulum stress and leads to autophagy by activating Ca^{2+}-mediated AMPK. Food Chem. Toxicol. 121, 648–656.

Jayasooriya, R.G., Choi, Y.H., Hyun, J.W., Kim, G.Y., 2014. Camptothecin sensitizes human hepatoma Hep3B cells to TRAIL-mediated apoptosis via ROS-dependent death receptor 5 upregulation with the involvement of MAPKs. Environ. Toxicol. Pharmacol. 38, 959–967.

Jayasooriya, R.G., Park, S.R., Choi, Y.H., Hyun, J.W., Chang, W.Y., Kim, G.Y., 2015. Camptothecin suppresses expression of matrix metalloproteinase-9 and vascular endothelial growth fatctor DU145 through PI3K/Akt-mediated inhibition of NF-kB activity and Nrf2-dependent induction of HO-1 expression. Environ. Toxicol. Pharmacol. 39, 118–1198.

Kim, H.S., Heo, J.I., Park, S.H., Shin, J.Y., Kang, H.J., Kim, M.J., Kim, S.C., Kim, J., Park, J.B., Lee, J.Y., 2014. Transcriptional activation of $p21^{WAF1/CIP1}$ is mediated by increased DNA binding activity and increased interaction between p53 and Sp1 via phosphorylation during replicative senescence of human embryonic fibroblasts. Mol. Biol. Rep. 41, 2397–2408.

Kim, Y.K., Koo, N.Y., Yun, P.Y., 2015. Anticancer effects of CKD-602 (Camtobell((R))) via G2/M phase arrest in oral squamous cell carcinoma cell lines. Oncol Lett 9, 136–142.

Kreis, N.N., Louwen, F., Yuan, J., 2015. Less understood issues: $p21^{Cip1}$ in mitosis and its therapeutic potential. Oncogene 34, 1758–1767.

Lin, P.Y., Fosmire, S.P., Park, S.H., Park, J.Y., Baksh, S., Modiano, J.F., Weiss, R.H., 2007. Attenuation of PTEN increases p21 stability and cytosolic localization in kidney cancer cells: a potential mechanism of apoptosis resistance. Mol. Canc. 6, 16.

Lindqvist, A., van Zon, W., Karlsson Rosenthal, C., Wolthuis, R.M., 2007. Cyclin B1-Cdk1 activation continues after centrosome separation to control mitotic progression. PLoS Biol. 5, e123.

Marston, A.L., Wassmann, K., 2017. Multiple duties for spindle assembly checkpoint kinases in Meiosis. Front Cell Dev Biol 5, 109.

Matthess, Y., Raab, M., Sanhaji, M., Lavrik, I.N., Strebhardt, K., 2010. Cdk1/cyclin B1 controls Fas-mediated apoptosis by regulating caspase-8 activity. Mol. Cell Biol. 30, 5726–5740.

Moon, D.O., Choi, Y.H., Kim, G.Y., 2011. Role of p21 in SP600125-induced cell cycle arrest, endoreduplication, and apoptosis. Cell. Mol. Life Sci. 68, 3249–3260.

Musacchio, A., 2015. The molecular biology of spindle assembly checkpoint signaling dynamics. Curr. Biol. 25, R1002–R1018.

Park, D.S., Morris, E.J., Greene, L.A., Geller, H.M., 1997. G_1/S cell cycle blockers and inhibitors of cyclin-dependent kinases suppress camptothecin-induced neuronal apoptosis. J. Neurosci. 17, 1256–1270.

Parrish, A.B., Freel, C.D., Kornbluth, S., 2013. Cellular mechanisms controlling caspase activation and function. Cold Spring Harb Perspect Biol 5.

Ribas, V.T., Goncalves, B.S., Linden, R., Chiarini, L.B., 2012. Activation of c-Jun N-terminal kinase (JNK) during mitosis in retinal progenitor cells. PLoS One 7 e34483.

Saitoh, S., Ishii, K., Kobayashi, Y., Takahashi, K., 2005. Spindle checkpoint signaling requires the mis6 kinetochore subcomplex, which interacts with mad2 and mitotic spindles. Mol. Biol. Cell 16, 3666–3677.

Senese, S., Lo, Y.C., Gholkar, A.A., Li, C.M., Huang, Y., Mottahedeh, J., Kornblum, H.I., Damoiseaux, R., Torres, J.Z., 2017. Microtubins: a novel class of small synthetic microtubule targeting drugs that inhibit cancer cell proliferation. Oncotarget 8, 104007–104021.

Shao, R.G., Cao, C.X., Shimizu, T., O'Connor, P.M., Kohn, K.W., Pommier, Y., 1997. Abrogation of an S-phase checkpoint and potentiation of camptothecin cytotoxicity by 7-hydroxystaurosporine (UCN-01) in human cancer cell lines, possibly influenced by p53 function. Cancer Res. 57, 4029–4035.

Tian, W., Li, B., Warrington, R., Tomchick, D.R., Yu, H., Luo, X., 2012. Structural analysis of human Cdc20 supports multisite degron recognition by APC/C. Proc. Natl. Acad. Sci. U. S. A. 109, 18419–18424.

Tsimberidou, A.M., Takimoto, C.H., Moulder, S., Uehara, C., Mita, M., Mita, A., Urban, P., Tan, E., Wang, Y., Vining, D., Kurzrock, R., 2011. Effects of patupilone on the pharmacokinetics and pharmacodynamics of warfarin in patients with advanced malignancies: a phase I clinical trial. Mol. Canc. Therapeut. 10, 209–217.

Wang, Y., Jin, F., Higgins, R., McKnight, K., 2014. The current view for the silencing of the spindle assembly checkpoint. Cell Cycle 13, 1694–1701.

Wong, H.W., Shaukat, Z., Wang, J., Saint, R., Gregory, S.L., 2014. JNK signaling is needed to tolerate chromosomal instability. Cell Cycle 13, 622–631.

Xiao, Z., Chen, Z., Gunasekera, A.H., Sowin, T.J., Rosenberg, S.H., Fesik, S., Zhang, H., 2003. Chk1 mediates S and G_2 arrests through Cdc25A degradation in response to DNA-damaging agents. J. Biol. Chem. 278, 21767–21773.

Yagdi Efe, E., Mazumder, A., Lee, J.Y., Gaigneaux, A., Radogna, F., Nasim, M.J., Christov, C., Jacob, C., Kim, K.W., Dicato, M., Chaimbault, P., Cerella, C., Diederich, M., 2017. Tubulin-binding anticancer polysulfides induce cell death via mitotic arrest and autophagic interference in colorectal cancer. Cancer Lett. 410, 139–157.

Zare-Mirakabadi, A., Sarzaeem, A., Moradhaseli, S., Sayad, A., Negahdary, M., 2012. Necrotic effect versus apoptotic nature of camptothecin in human cervical cancer cells. Iran. J. Cancer Prev. 5, 109–116.

Zeng, C.W., Zhang, X.J., Lin, K.Y., Ye, H., Feng, S.Y., Zhang, H., Chen, Y.Q., 2012. Camptothecin induces apoptosis in cancer cells via microRNA-125b-mediated mitochondrial pathways. Mol. Pharmacol. 81, 578–586.

Zeng, X., Sigoillot, F., Gaur, S., Choi, S., Pfaff, K.L., Oh, D.C., Hathaway, N., Dimova, N., Cuny, G.D., King, R.W., 2010. Pharmacologic inhibition of the anaphase-promoting complex induces a spindle checkpoint-dependent mitotic arrest in the absence of spindle damage. Cancer Cell 18, 382–395.